Structural Engineering and Mechanics, *Vol. 53, No. 1 (2015) 73-87*
DOI: http://dx.doi.org/10.12989/sem.2015.53.1.073

Crash analysis of military aircraft on nuclear containment

M.R. Sadique*, M.A. Iqbal[a] and P. Bhargava[b]

Department of Civil Engineering, Indian Institute of Technology Roorkee, Roorkee-247667, India

(Received November 5, 2013, Revised May 27, 2014, Accepted July 6, 2014)

Abstract. In case of aircraft impact on nuclear containment structures, the initial kinetic energy of the aircraft is transferred and absorbed by the outer containment, may causing either complete or partial failure of containment structure. In the present study safety analysis of BWR Mark III type containment has been performed. The total height of containment is 67 m. It has a circular wall with monolithic dome of 21m diameter. Crash analysis has been performed for fighter jet Phantom F4. A normal hit at the crown of containment dome has been considered. Numerical simulations have been carried out using finite element code ABAQUS/Explicit. Concrete Damage Plasticity model have been incorporated to simulate the behaviour of concrete at high strain rate, while Johnson-Cook elasto-visco model of ductile metals have been used for steel reinforcement. Maximum deformation in the containment building has reported as 33.35 mm against crash of Phantom F4. Deformations in concrete and reinforcements have been localised to the impact region. Moreover, no significant global damage has been observed in structure. It may be concluded from the present study that at higher velocity of aircraft perforation of the structure may happen.

Keywords: nuclear safety; containment buildings; aircrafts crash; Phantom f4

1. Introduction

Radioactive releases due to failure of nuclear containment structure can cause worst category of disaster to human life and earth environment. It could be more severe than a big earthquake or a large dam failure, as it can cause disastrous after effects for generations. The nuclear containment structures provide biological and nuclear shielding to limit the radiation dose to the atmosphere in cases of accidents. The outer containment structure is made up of concrete to protect the inner containment from any external impact as well as it provides an additional protection to prevent the leakage of radiation to the human atmosphere. In long term nuclear energy is the cheapest energy source available. Due to it, in spite of all the negative effects concerned with nuclear energy, its demand is always on escalation.

Majority of containment buildings are located in the countries which have hectic air traffic. Hence, vulnerability of containment buildings against accidental or deliberate crash of aircrafts is always in apprehension. Researches on safety analysis of containment structures against aircraft crash evolved through last five decades. Earlier studies contains analytical calculations with lots of

*Corresponding author, Ph.D., E-mail: rehan.sadique@gmail.com
[a]Ph.D., E-mail: iqbal_ashraf@rediffmail.com, iqbalfce@iitr.ernet.in
[b]Ph.D., E-mail: bhpdpfce@iitr.ernet.in

http://www.techno-press.org/?journal=sem&subpage=8 ISSN: 1225-4568 (Print), 1598-6217 (Online)

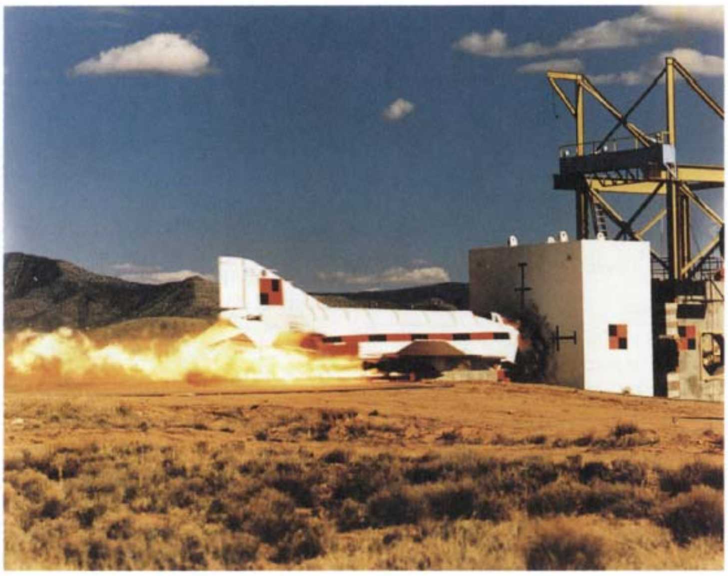

Fig. 1 Phantom F4 striking RCC wall (Sugano *et al*. 1993)

assumptions and hypothesis (Riera 1968, Drittler and Gruner 1976, Bahar and Rice 1978) uncoupled analysis using estimated reaction time response of aircrafts and basic finite element programming (Yang and Godfrey 1970, Riera 1980, Paul *et al.* 1993, Gomathinayagam *et al.* 1994, Abbas *et al.* 1995, 1996). Use of reaction time response curves of aircrafts to analyse the response of containment building has been widely accepted in literature and known as "Riera Approach". Moreover, the solitary available experimental study of aircraft crash problem (see Fig. 1) suggests that existing "Riera Approach", with minor adjustment, is a practical way of evaluating the impact force (Sugano *et al.* 1993). In the last decade, scenario is entirely modified with availability of sophisticated finite element code (ADINA, ABAQUS, LS-DYNA etc.), high resolution cameras and efficient computational facilities. Availability of these technologies facilitated modern researchers to evaluate effects of concrete strength (Hu and Chou 2002, Werner 2010), wall thickness and reinforcements (Katayama *et al.* 2004, Lo Frano and Forasassi 2011a), strain rate (Iqbal *et al.* 2012) etc., in the aircraft crash problem. It has been found through geometric modelling of aircrafts body and containment building that with "Riera Approach" the results may be quite sensitive to the assumptions associated with loading area and timing of load application (Arros and Doumbalski 2007).

The important point to be highlighted here is that majority of these studies had been confined to a particular location i.e., the junction of dome and cylinder of the containment building. Only Abbas *et al*. (1996) considered a crash of Boeing 707-320 on the dome of the containment. However, the aircraft discussed by Abbas *et al*. (1996) has now been obsolete. Kukreja (2005) observed the displacements at crown of the containment, but not considered it as impact location. Nevertheless, due to height and massiveness of containment structure, its dome portion is most exposed surface to aircraft crash threat. Hence, in the present study, the crown of containment dome has been considered as the impact location. A direct hit has been assumed to find out the response of containment against the crash load. Fighter jet Phantom F4 aircrafts has been chosen to check the stability of containment dome against crash of aircrafts.

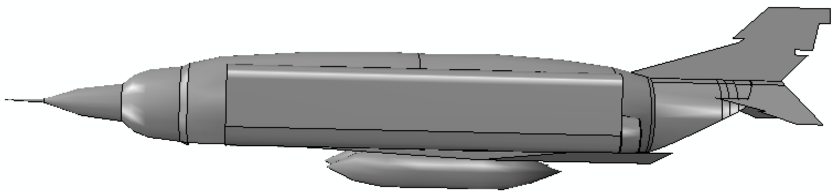

Fig. 2 Schematic image of Phantom F4

Table 1 Brief specification of Phantom F4

Wingspan:	11.71 m
Length:	17.75 m
Height:	5 m
Ceiling:	17 Km
Range:	Around 3000 Km
Weight:	25,000 kg
Maximum Speed:	663 m/s (max.)
Speed considered:	215 m/s

2. Aircraft loading

Military aircrafts are fast and highly maneuverable. Among military aircrafts, fighter aircrafts are designed primarily for air-to-air combat against other aircraft. Fighter jet Phantom F4 has been selected in the present study to find out the response of containment against aircraft crash. The Phantom F-4, with top speeds more than twice that of sound, was one of the most versatile fighters ever built, see Fig. 2. The Phantom F4 had made its entry in military services in early sixties. The F-4 Phantom emerged as a multipurpose strike bomber dexterous enough to prevail in any type of air combat, hence, quickly adopted by the USAF and Marine Corp and became one of the mainstay aircraft in numerous air forces around the world. Phantom F4 is capable of pushing Mach 2 (680 m/s) at altitude, had an operational upper limit of over 21 Km depending on the version and could carry more than 7000 kg ordnance externally. Several hundred of this jet was still in service, nearly 60 years after its first flight. Brief specification of the aircraft has been given in Table 1, (Lo Frano and Forasassi 2011b).

In the present study, the loading of the aircraft to the containment has been assigned through the reaction-time response curves of the aircraft. Reaction time response curve of Phantom F4 has been calculated for three different velocities i.e., Mach 1 (340m/s), Mach 0.735 (250 m/s) and Mach 0.632 (215 m/s) using the interface reaction equation discussed in Sadique *et al.* (2013), Fig. 3. It can be noticed that the increase in speed from 0.6 Mach to 1 Mach has enhanced the peak impact force more than 2.5 times and decreased the impact duration from 0.08 sec to 0.05 sec. In conventional design, response of containment had been analyzed by using the reaction time curve of the Phantom F4 at a speed of 215 m/s. Moreover, the same speed has been considered in the full scale impact test conducted by Sugano *et al.* (1993). Hence, in the present study also the reaction time curve for 215 m/s speed has been incorporated as impact load of the aircraft. Nevertheless, it has to be understood that in case of deliberate attack the aircraft may hit the target with higher speed, consequently, may cause more disastrous effect than that quantified in the present study.

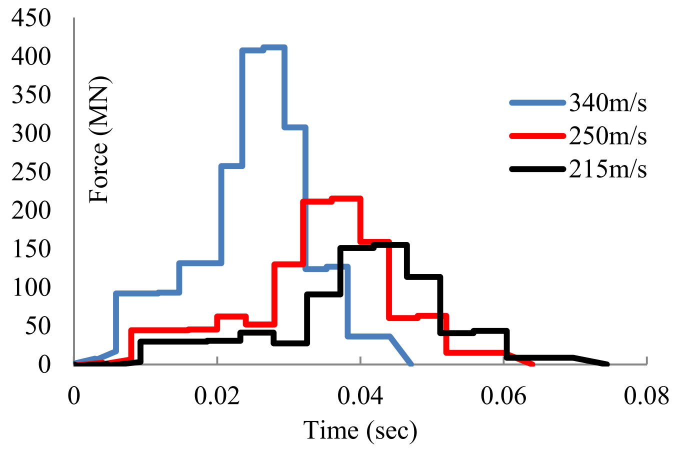

Fig. 3 Reaction time response of Phantom F4 at different velocities

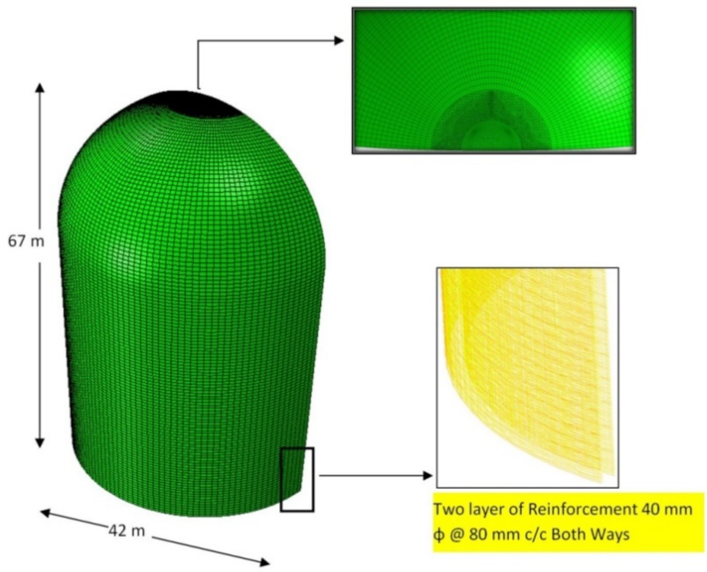

Fig. 4 Containment building and reinforcement detailing

The loading of aircraft was assigned to the containment at a constant contact area equivalent to the average of total cross-sectional area of fuselage and wings of the aircraft. It should be elaborated here, that in order to simplify the problem, instead of providing a bird-shaped contact area; a circular area has been assumed in the present study. In the available literature Gomathinayagam *et al*. (1994), Abbas *et al*. (1995, 1996), Kukreja (2005), Lo Frano anf Forasassi (2011a), Iqbal *et al.* (2012) had followed the same hypothesis in the assumption of contact area for impact loading of aircraft. Accordingly, the impact zone of Phantom F4 was considered as a circular region of ø6 m. The reaction force was thus converted into pressure, after dividing with the magnitude of the contact surface area. The calculated time varying pressure has been assigned to the impact location, depicted in Fig. 4.

3. Modelling of containment

In nuclear power reactors, containment systems have variation by size, shape, materials used, and suppression systems. The kind of containment used is determined by the class of reactor and the specific plant needs. The outer containment of a typical BWR Mark III type containment has been considered in the present study. BWR Mark III is modern evolved model of Boiling Water Reactors (BWR) nuclear power plants. This similar containment has been studied by Abbas *et al*. (1995, 1996) for the impact of Boeing 707-320. The containment has a semi-spherical dome of 42 m inner diameter supported on circular wall of same diameter having 46 m height, hence having a total height of 67 m. The wall and dome of the containment building has a uniform thickness of 1.2 m throughout. The reinforcement has been modelled as Ø 40 mm bars at 80 mm centre to centre both ways at the inner and outer faces of the cylindrical wall as well as the spherical dome, Fig. 4. A 100 mm effective concrete cover has been specified. Base of the nuclear containment is assumed to be fixed. Moreover, considering the symmetry in the containment building only half of the containment has been modelled.

4. Finite element model

The containment structure has been meshed mainly with 3D stress element C3D8R (Continuum three dimensional reduced integration eight node), see Fig. 4. To perform the analysis within the limited time frame, only the area of impact has been divided in ten layers. However remaining part of the containment has divided only in two layers. Aspect ratio of elements has been kept unity. In impact analysis problem through the finite element methods moderate aspect ratios has been preferred. With high aspect ratio the possibility of element distortion becomes large and computational accuracy were lost. Hence, in order to maintain higher accuracy, the aspect ratio of the elements in the analysis should be as close to unity as possible. Moreover, there has been an intermediate layer of 4 node linear tetrahedral elements (C3D4). This region was considered to

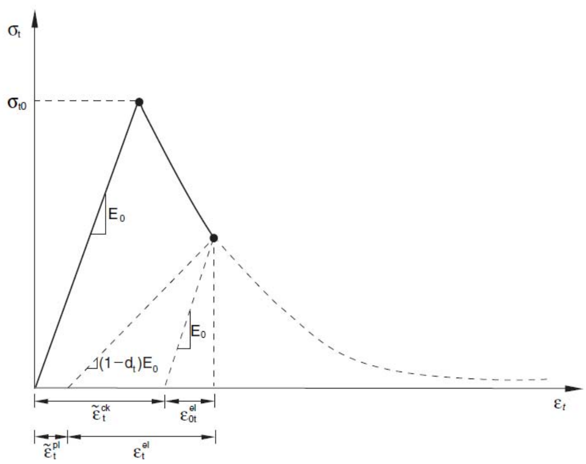

(a)

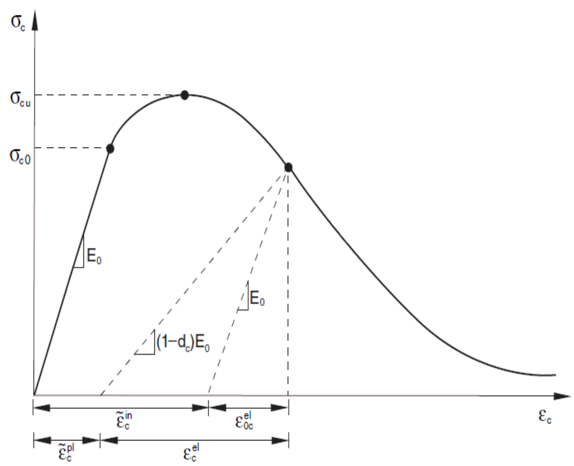

(b)

Fig. 5 Behavior of concrete under uniaxial loading: (a) tension (b) compression (ABAQUS manual 2008) maintain the compatibility between the meshes of impact region and outer region. The mesh convergence was studied by varying the size of concrete element as 150 mm×150 mm×150 mm, 120 mm×120 mm×120 mm and 100 mm×100 mm×100 mm in the impact region of the containment against crash of Boeing 707-320 aircraft. The maximum nodal deformation in the impact region was found to be 90.82 mm, 89.96 mm and 89.6 mm respectively. The reinforcement steel bars have been modelled using a 2 node three dimensional truss element (T3D2) of 600 mm length throughout the containment along the circumferential and meridonial directions. There are a total 514640 elements in the present model with 501803 nodes.

5. Constitutive material models

To study the response of significantly important reinforced concrete structure through finite element simulations is a complex task, especially in sensitive environments like nuclear power plants where the experimental studies are really difficult. Selection of proper boundary conditions, mesh size, element type and a precisely valid constitutive material model are one of the important parts of the analysis. However, constitutive material models for concrete as well as reinforcements under high strain loading have not much variety of options. In a recent study, three different models of damage for the concrete at high strain loading viz. (i) concrete smeared cracking model, (ii) concrete damaged plasticity model and (iii) concrete brittle cracking model had been compared numerically by Martin (2010). It was concluded that the concrete damage plasticity (CDP) model includes hardening as well as softening in the post elastic response of concrete and has been found to be most suitable for impact problems. The CDP model available in ABAQUS is a revision of the Drucker-Prager strength hypothesis wherein the scalar isotropic damage has been introduced later by several researchers (Kachanov 1958, Rabotnov 1969, Lubliner *et al.* 1989, Lee and Fenves 1998).

In the present study CDP model has been used to incorporate the material behaviour of concrete. The stress-strain relationship under uniaxial tension follows linear elastic relationship until the attainment of failure stress (σ_{t0}) which corresponds to the onset of micro-cracking in the concrete, Fig. 5(a). Beyond failure stress, the formation of micro-cracks is represented macroscopically with a softening stress-strain response. The stress-strain relationship under uniaxial compression is linear until the attainment of initial compressive strength, σ_{c0}, Fig. 5(b). In the plastic region however, the response up to ultimate stress (σ_{cu}), is characterized by stress hardening, followed by the strain softening. The concrete specimen when unloaded from any point on the strain softening branch shows degradation of the elastic stiffness which has been characterized in the model by the tension and compression damage variables, d_t and d_c respectively. The stress-strain relations under uniaxial tension and compression are governed by the following expressions respectively (ABAQUS Manual)

$$\sigma_t = (1 - d_t)E_0\,(\varepsilon_t - \tilde{\varepsilon}_t^{pl}) \tag{1}$$

$$\sigma_c = (1 - d_c)E_0\,(\varepsilon_c - \tilde{\varepsilon}_c^{pl}) \tag{2}$$

Where σ and ε is the total stress and strain respectively, subscripts t and c refer to tension and compression respectively, d is the damage variable, $\tilde{\varepsilon}_t^{pl}$and $\tilde{\varepsilon}_c^{pl}$ are the equivalent plastic strains, and E_0 is the elastic modulus of the undeformed concrete.

However, Johnson-Cook elasto-visco plastic model has been used to incorporate the material behaviour of reinforced steel. A detail discussion of material model of concrete as well as reinforcement can be found in our previous work Sadique *et al*. (2013). However, in the present study, behaviour of fighter plane crash has been considered as hard impact. Hence, considering the strain rate range given by Pajak (2011), stress versus strain curve of concrete has been used for constant strain rate of 620s^{-1} only. However, material properties of concrete have been provided in Table 2 and properties of reinforcement steel used in the analysis has been illustrated in Table 3.

Table 2 Material properties for concrete

Density, ρ (kg/m^3)	2400
Modulus of elasticity, E (N/m^2)	2.7386E+10
Poisson's ratio, ϑ	0.17
Dilation angle, ψ	30
Eccentricity	1.0
Initial equi-biaxial compressive yield stress to initial uniaxial compressive yield stress, f_{b0}/f_{c0}	1.16
Bulk Modulus, K	0.666
Fracture Energy, G_f(N/m)	720
Uniaxial Failure Stress (Tension), σ_{t0} (MPa)	10.8
Cracking displacement, U_{to} (m)	0.0001332
Tensile strength, $\sigma_{st,}$ MPa	3.86
Compressive Strength, MPa	25.8

Table 3 Material properties for reinforcing steel, (Borvik *et al.* 2002)

Young's modulus; E (N/ mm^2)	2×10^5
Poisson Ratio, ϑ	0.33
Density, ρ (kg/m^3)	7850
Yield stress, A (N/mm^2)	490
B (N/ mm^2)	383
n	0.45
Reference strain rate, $\dot{\varepsilon}$ (s^{-1})	5x10^{-4}
C	0.0114
m	0.94
T_{melt} (K)	1800
T_0 (K)	293
Specific heat Cp (J/kg K)	452
Inelastic heat fraction, α	0.9
D_1	0.0705
D_2	1.732
D_3	-0.54
D_4	-0.01
D_5	0.0

6. Results and discussions

Finite element code ABAQUS/Explicit has been used to carry out numerical simulations wherein fighter jet Phantom F4 has been considered to hit the outer containment of the BWR Mark III type nuclear power plant. The location of the impact was considered at the crown of dome and the angle of incidence 90° (normal to the surface). The probability of perpendicular strike of a fighter jet on the containment dome is quite low, however the deformation caused in this case will be highest compared to any oblique impact. A comparative discussion of oblique and normal impact can be found in Abbas (1992). The local as well as global deformations of the structure were measured and the stresses in the concrete and reinforcement were evaluated.

The maximum deformation in the concrete is about 35.26 mm. Deformations are highly concentrated in area of crash; see Fig. 6(a). Maximum deformation has been reported at 0.05 sec after impact. The set of reinforcements at inner face has maximum deformation of 33.67 mm, while outer set of reinforcement is bearing a maximum deformation of approx. 20 mm, as shown in Fig. 6(b) and 6(c). The inset provided in Fig. 6(a), (b), (c) are showing the deformation contour of loading surface. It can be seen that deformation at reinforcement facing inner face of containment is quite higher than that of outer facing reinforcement. Further, outer and inner face has been elaborated in Fig. 7(a).

To observe the pattern of deformation and other parameters more clearly, a vertical axis passing through centre of impact region and another path along each face has been selected, as shown in Fig. 7(a). Elements of three different locations have been chosen to plot the response of reinforcements, see Fig. 7(b). Observations have been reported along the depth, at three different timing i.e., @ 0.04 sec, 0.05 sec and 0.06 sec after the impact started. It can be noticed from Fig. 8(a), that there has been almost equal deformation throughout the depth axis of containment up to 0.04 sec. As the peak load arrives at 0.05 sec, deformation has been raised drastically. Moreover, difference in the deformation at both faces can be clearly noticed. At the outer face deformation is near 20 mm, while at the inner face it is 35 mm approximately. Containment structure regains the elastic deformations at 0.06 sec when impact load turn out to be lesser. The amount of plastic strain has been found to be more significant near the inner face at all three time steps, see Fig. 8(b). Nevertheless, elements near the outer face have been facing negligible plastic strain.

The stress component in the direction of loading along the depth axis has been plotted in Fig. 8(c). The positive sign shows tension while the negative sign compression. In the initial stage, outer face is in compression and the inner face of the containment is under tension, due to vertical download loading. However, at the peak load stress near outer face has been raised up to 20 MPa in compression. Finally at 0.06 sec stresses at both the face has been changing its direction, due to the elastic recover of deformation. Plots of Von Mises stress distribution along the thickness of the containment dome have been shown in Fig. 8(d). Von Mises stress is used in determining whether an isotropic material will yield when subjected to a complex loading condition. Von Mises stress is a geometrical combination of all the normal and shear stress components in the three directions, acting at a particular location. Stresses are released at inner face because of higher deformation near this face.

The damage of the concrete under tension or compression forces has been assumed to occur when the corresponding damage parameter, d_t or d_c respectively, has reached a value of 0.9. The value of the damage parameter varies from 0 to 0.9 for undamaged and complete damaged material respectively. The compression failure is found to be very negligible, therefore no results has been mentioned here. The tension damage of concrete has been found to occur at the inner face

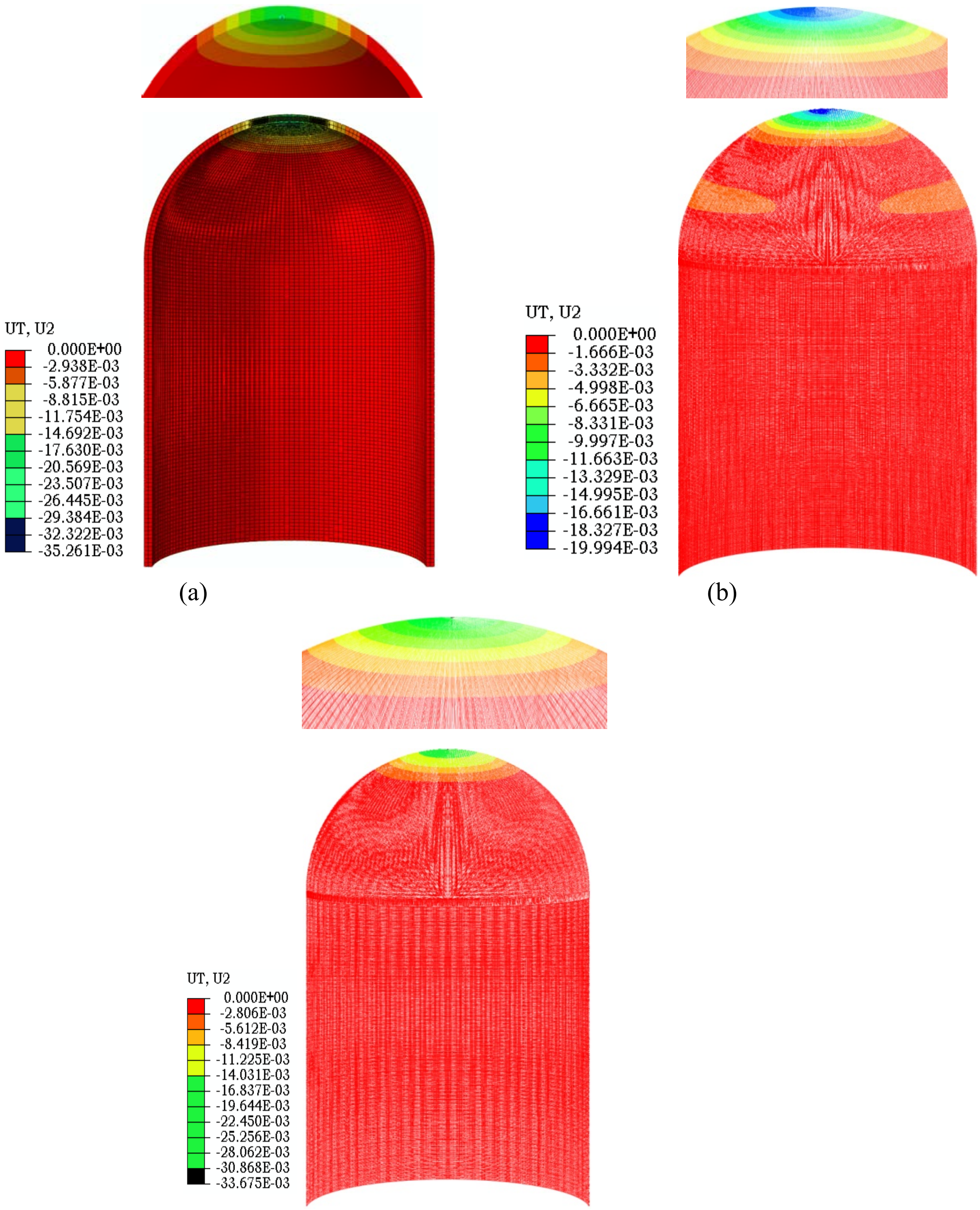

Fig. 6 Maximum deformation in (a) concrete (b) reinforcement facing outer face (c) reinforcement facing inner face

of the impact region of the containment, Fig. 8(e). However only few elements have found to be reaching the damage value close to 0.9 i.e., no element of concrete is fully damaged. Hence, it may be concluded that probability of scabbing of concrete cover on the inner face of containment were higher. Any other robust material model may show the smearing of concrete at this stage.

To observe the extension of the deformation along each face two axis has been selected as shown in Fig. 7(a). It has been observed that deformation along the both face is almost equal except near the centre of impact, see Fig. 9(a). This phenomenon may be regarded as punching shear failure with scabbing of concrete at the inner face. The scabbing of concrete at the inner face of containment may be due to stress wave response (Martin 2010). Variation of principle stress along the direction of loading at both faces has been shown in Fig. 9(b).

Central element of impact region has been chosen to plot the time dependent deformation in concrete at each face. It has to be noticed that deformation at both faces has equal value (17 mm) up to 0.04 sec. After that there is relatively higher deformation at the inner face, as mentioned earlier also. Near the end of curve, when impact load turn out to be lesser, an elastic rebound has been noticed, see Fig. 10(a). Moreover, there has been a nominal outward deformation at outer face due to elastic rebound of the containment structure. However, graph of principal stress at these two elements shows entirely different characteristics as shown in Fig. 10(b). A sinusoidal pattern of tension and compression stress has been found throughout the impact.

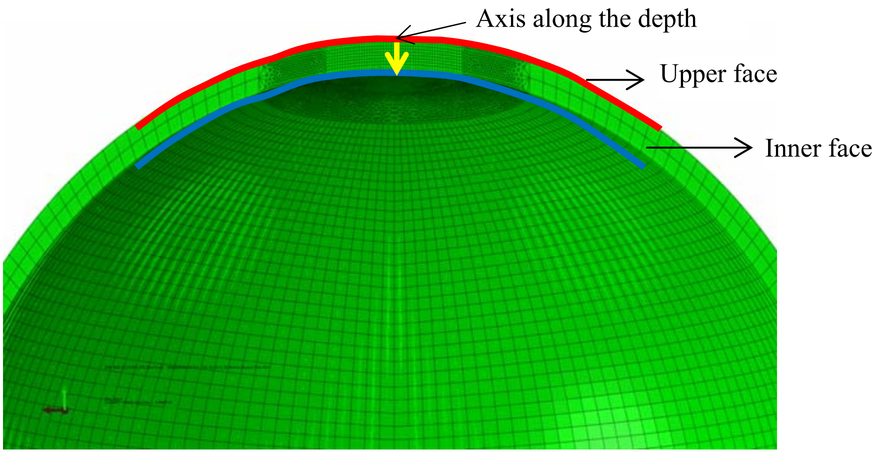

Fig. 7 (a) Axis and path selected to observe the response

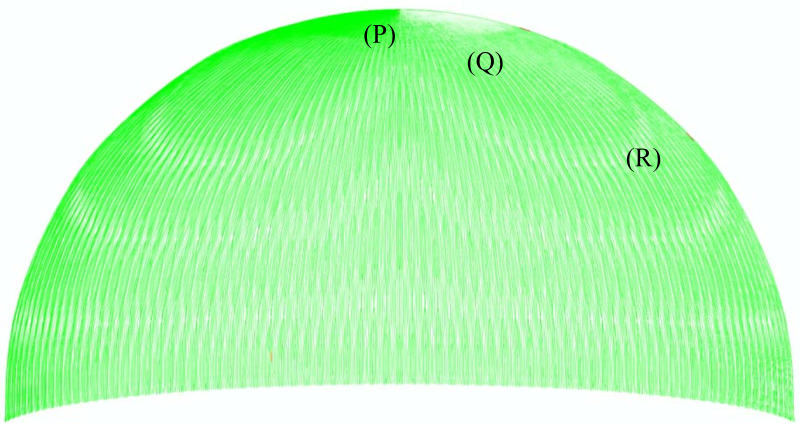

Fig. 7 (b) Elements selected at different locations of reinforcements to display results

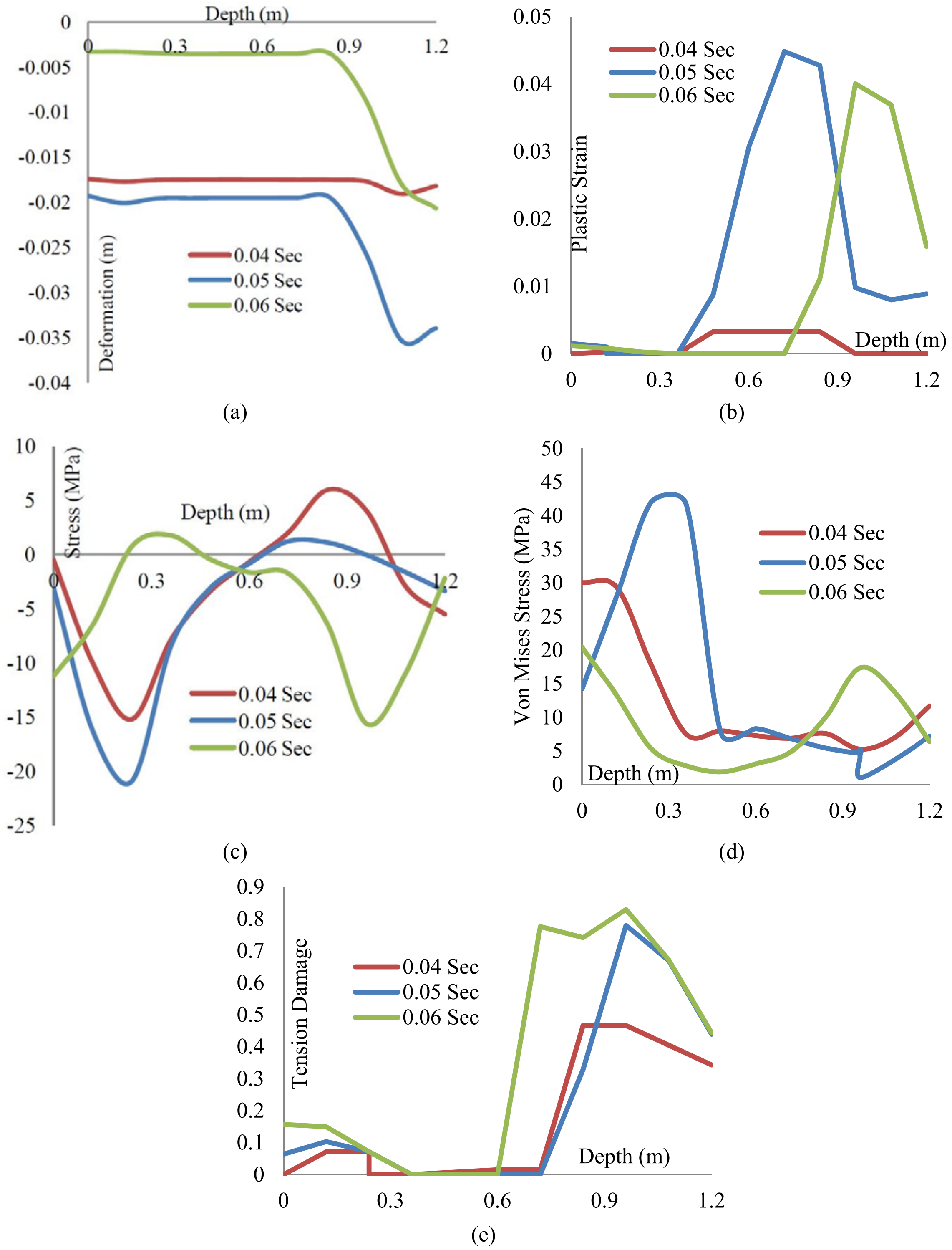

Fig. 8 Variation along the thickness of containment in impact region in concrete elements (a) deformation (b) plastic strain (c) stress along the direction of loading (d) von-Mises stress (e) tension Damage

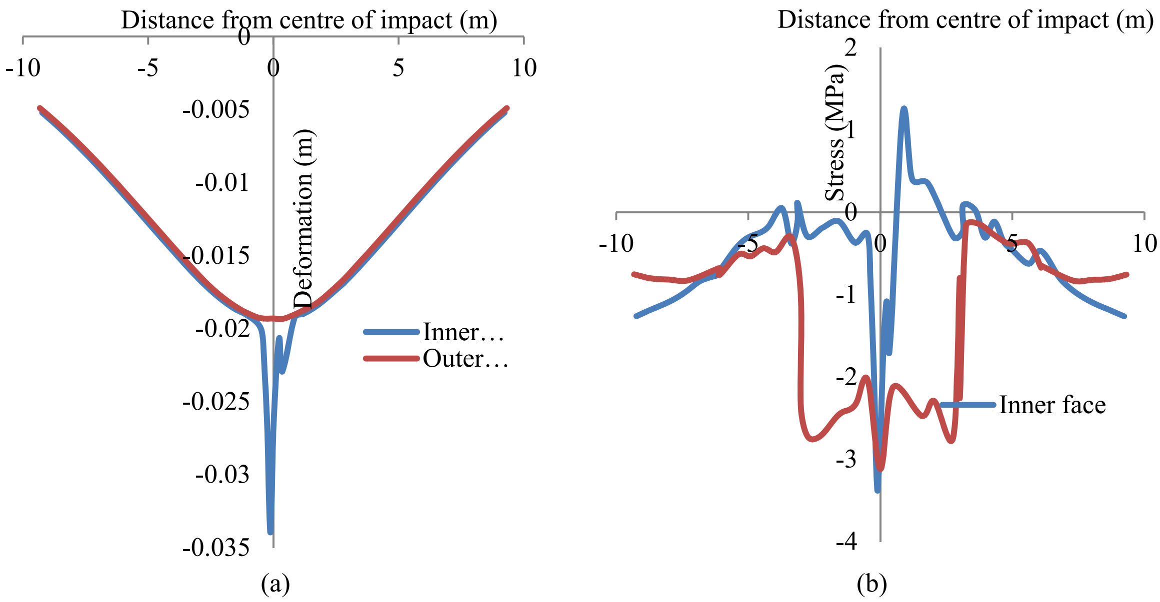

Fig. 9 Variation along the inner and outer face of containment in impact region (a) deformation (b) principal stress

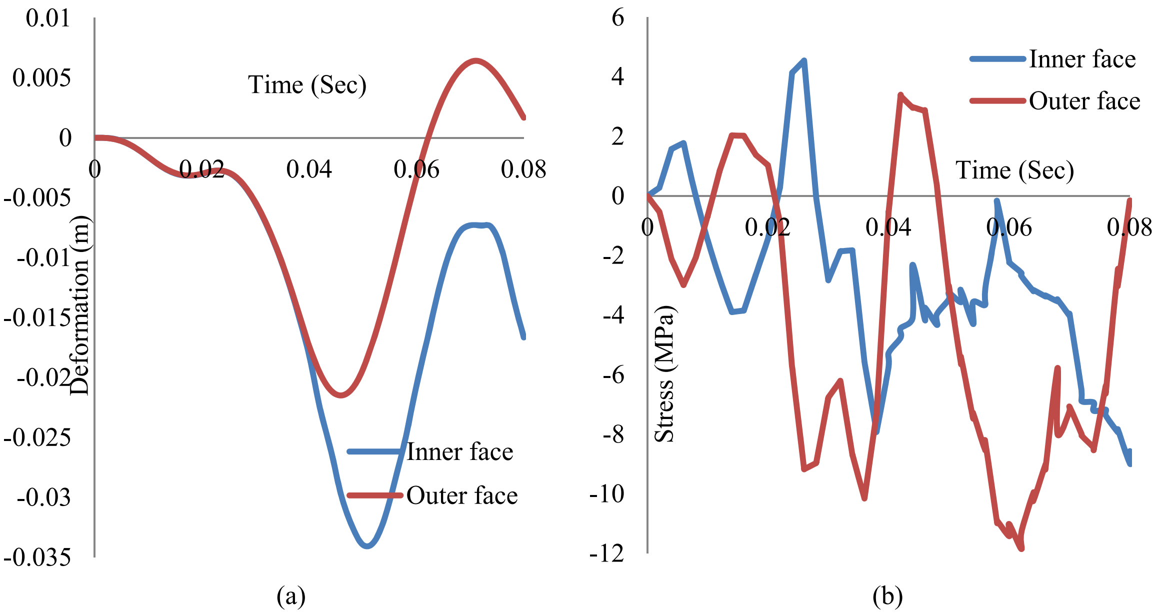

Fig. 10 Response of central element of impact region at outer and inner face (a) deformation v/s time (b) stress v/s time

Behaviour of reinforcement elements has also been plotted for three different locations, as shown in Fig. 7(b). At location *P* i.e., impact location outer set of reinforcement is under

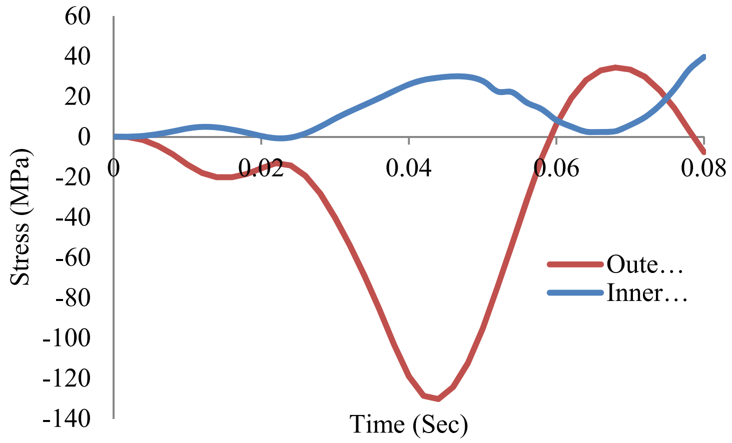

(a)

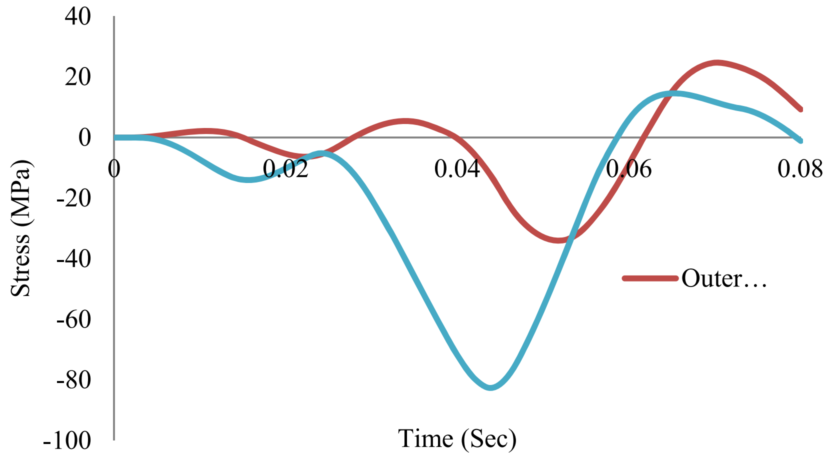

(b)

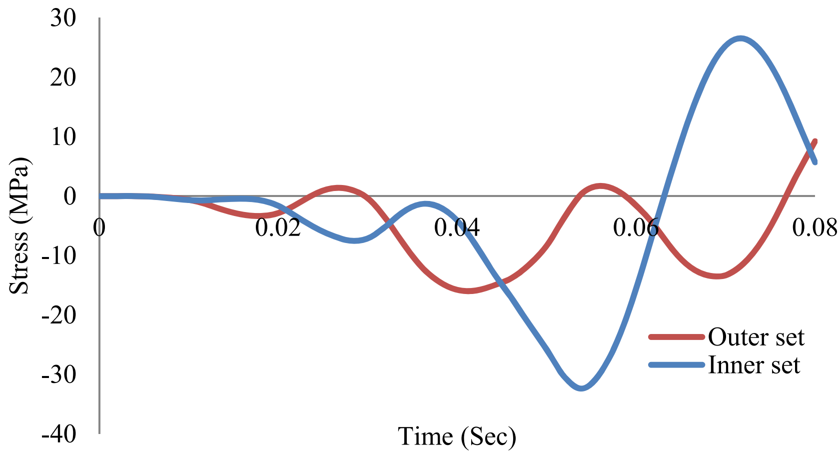

(c)

Fig. 11 Stress v/s time response of outer and inner set of reinforcement element at (a) location P (b) location Q (c) location R compression. 135 MPa compressive stress has been noticed, which far less than yield stress of the reinforcement. Moreover there is a small tensile stress of 20 MPa in inner set of reinforcement. As going away from impact region compressive stress are dominating at both set of reinforcement, see Fig. 11 (a), (b), (c). There has nominal tensile stress at the end of impact, which is mainly due to elastic rebound of containment structure.

7. Conclusions

The response of the outer containment of BWR Mark-III type nuclear power plant has been studied against crash of fighter aircraft Phantom F4. Finite element analysis has been carried out using ABAQUS/ Explicit. The location of impact was considered at crown of the containment and the angle of incidence normal to the surface. The maximum local deformation in the containment wall was found to be approximately 35 mm against crash of Phantom F4. The set of reinforcement facing outer face of the containment has higher deformation than that of inner face. Severe local damage has been observed, however, structure is globally stable. Due to consideration Concrete Damaged Plasticity (an elasto-plastic material model), structural rebound has been noticed at plummeting of the impact load. A punching failure type phenomenon has been observed at the inner face of containment structure. As that the increase in velocity from 0.6 Mach to 1 Mach would enhance the peak impact force about 2.5 times. An interpretation may be drawn from current results that the aircraft may perforate the structure if hits with a higher speed.

References

Abbas, H., Paul, D.K., Godbole, P.N. and Nayak, G.C. (1995), “Reaction time response of aircraft crash”, *Comput. Struct.*, **55**(5), 809-817.

Abbas, H., Paul, D.K., Godbole, P.N. and Nayak, G.C. (1996), “Aircraft crash upon outer containment of nuclear power plant”, *Nucl. Eng. Des.*,**160,** 13-50,

Arros, J. and Doumbalski, N. (2007), “Analysis of aircraft impact to concrete structures”, *Nucl. Eng. Des.*, **237**, 1241-1249.

Drittler, K. and Gruner, P. (1976), “The force resulting from impact of fast-flying military aircraft upon a rigid wall”, *Nucl. Eng. Des.*, **37**, 245-48.

Gomathinayagam, S., Dharaneepathy, M.V. and Keshava Rao, M.N. (1994), “Damage-zones of containment structures under aircraft impact loads”, *Comput. Struct.*, **52**(3), 581-590.

Iqbal, M.A., Rai, S., Sadique, M.R. and Bhargava, P. (2012), “Numerical simulation of aircraft crash on nuclear containment structure”, *Nucl. Eng. Des.*, **243**, 321-335.

Kachanov, L.M. (1958), “On creep rupture time”, *Izvestiya Akademii Nauk SSSR, Otdeleniya Tekhnicheskikh I Nauk*, **8**, 26-31.

Katayama, *et al*. (2004), “Numerical simulation of jumbo jet impacting thick concrete walls-effect of reinforcement and wall thickness”, *ACHPR-2*, Nara, Japan.

Kukreja, M. (2005), “Damage evaluation of 500MWe Indian Pressurized Heavy Water Reactor nuclear containment for aircraft impact”, *Nucl. Eng. Des.*, **235**, 1807-1817.

Lee, J. and Fenves, G.L. (1998), “Plastic-damage model for cyclic loading of concrete structures”, *J. Eng. Mech.*, **124**(8), 892-900.

Lo Frano, R. and Forasassi, G. (2011a) “Preliminary evaluation of aircraft impact on a near term nuclear power plant”, *Nucl. Eng. Des.*, **241**, 5245-50.

Lo Frano, R. and Forasassi, G. (2011b), ”Global structural response of an SMR reactor subjected to an

aircraft impact”, *ASME 2011 Small Modular Reactors Symposium, SMR 2011* , 387-394.
Lubliner, J., Oliver, J., Oller, S. and Oñate, E. (1989), “A plastic-damage model for concrete”, *Int. J. Solid. Struct.*, **25**, 299-329.
Martin, O. (2010), “Comparison of different Constitutive Models for concrete in ABAQUS/ Explicit for Missile Impact Analysis”, *Safety of present Nuclear Reactor Unit* (SPNR) EUR 24151 EN-(2010).
Pajak, M. (2011), “The influence of strain rate on the strength of concrete taking into account the experimental techniques”, *Arch. Civil Eng. Envir.*, **3**, 77-86.
Paul, D.K., Abbas, H., Godbole, P.N. and Nayak, G.C. (1993), “Aircraft crash upon a containment structure of a nuclear power plant”, *SMiRT-12*, J06/5.
Rabotnov, Y.N. (1969), *Creep problems in structural members*, North-Holland, Amsterdam.
Rice, J.S. and Bahar, L.Y. (1978), “Simplified derivation of the reaction-time history in aircraft impact on a nuclear power plant”, *Nucl. Eng. Des.*, **49**, 263-268.
Riera, J.D. (1968), “On the stress analysis of structures subjected to aircraft hnpact forces”, *Nucl. Eng. Des.*, **8**, 415-426.
Riera, J.D. (1980), “A critical reappraisal of nuclear power plant safety against accidental aircraft impact”, *Nucl. Eng. Des.*, **57**, 193-206.
Sadique, M.R., Iqbal, M.A. and Bhargava, P. (2013), “Nuclear containment structure subjected to commercial and fighter aircraft crash”, *Nucl. Eng. Des.*, **260**, 30-46.
Sugano, T., Tsubota, H., Kasai, Y., Koshika, N., Orui, S., Riesemann, W.A.V., Bickel, D.C. and Parks, M.B. (1993), “Full-scale aircraft impact test for evaluation of impact force”, *Nucl. Eng. Des.*, **140**, 373-385.
Yang, H.T.Y. and Godfrey, D.A. (1970), “Structural analysis of aircraft impact on a nuclear containment vessel and associated structures”, *Nucl. Eng. Des.*, **11**, 295-307.

CC